Modern Chemistry
2025, Vol. 13, No. 3, pp. 53-63
https://doi.org/10.11648/j.mc.20251303.12

Research Article

Green Synthesis of Magnetite: Characterization and Comparison with Conventional Chemical Methods

Asma Siddiqa[1], Halima Khatun[2], Golam Mostafa[1, *]

[1]Institute of Environmental Science, University of Rajshahi, Rajshahi, Bangladesh
[2]BCSIR Rajshahi Laboratories, Bangladesh Council of Scientific and Industrial Research (BCSIR), Rajshahi, Bangladesh

Abstract

Iron oxide nanomaterials have gained scientific focus for environmental remediation. This study aimed to compare the structural properties of magnetite using chemical and green synthesis methods, applying XRD, FT-IR, SEM, EDS, TGA, DLS, and zeta potential characterization techniques. The XRD analysis showed that the average particle size of chemical and green-synthesized magnetite was 11nm and 8.4nm, respectively. FT-IR analysis of green-synthesized magnetite showed the shifting of stretching vibration of C=O and C-O in green-synthesized magnetite from 1646 cm^{-1} to 1644 cm^{-1} and 1052 cm^{-1} to 1065 cm^{-1} after capping with leaf extract SEM images of green-synthesized magnetite was found to have some extent of aggregation due to the capping and stabilizing action of (e.g., polyphenols, flavonoids), present in leaf extract influence the nucleation and growth process during synthesis. The bio-organic matrix likely leads to steric hindrance and variation in crystal growth, resulting in less-defined shapes and reduced aggregation compactness. The EDS spectrum of green synthesized confirmed the existence of biomolecules (C). The hydrodynamic diameters were 150nm for green-synthesized and 158nm for chemically synthesized magnetite, while zeta potential was found to be -50 mV and -47 mV, respectively. This study demonstrated improved crystallinity and enhanced stability of green-synthesized magnetite compared to chemically synthesized magnetite. Therefore, the environmentally sustainable green synthesis method offers a promising alternative to the synthesis of magnetite for environmental applications.

Keywords

Capping Agent, Comparative Study, Green Synthesis, Jackfruit Leaf Extract, Magnetite Nanoparticle, Reducing Agent

1. Introduction

The Earth's atmosphere is being degraded result from rapid industrialization, urbanization, and population growth, which is exposing a significant number of hazardous and unwanted substances [1, 2]. Nanoscience and nanotechnology have gained much attention in the scientific world for sustainable environmental remediation [3, 4]. Science nanomaterials are highly reactive due to their shape, size, greater surface area, and uniform distribution, making them a potential competitor in environmental remediation like water treatment processes [5, 6].

Due to unique physicochemical characteristics, magnetic nanomaterials have attracted much interest in nanotechnology [7], and magnetite is one of them. The widespread implementation of magnetite nanoparticles in environmental remediation, industrial application, and bioengineering sectors is caused by their chemical stability, low cost, nontoxicity,

*Corresponding author: mgmostafa@ru.ac.bd (Golam Mostafa)

Received: 17 June 2025; **Accepted:** 2 July 2025; **Published:** 23 July 2025

good magnetic properties, and favorable adsorption properties [8]. Due to the growing demand for magnetite nanoparticles (NPs), researchers have proposed a synthetic method that is both environmentally friendly and inexpensive, as opposed to conventional physical and chemical synthesis methods [9]. Magnetite nanoparticles are usually synthesized using various techniques, such as co-precipitation, sol-gel, thermal breakdown, hydrothermal, microwave, ultra-sonication, combustion, vapor-solid growth, and micro emulsion [10]. The mentioned procedures, however, are rather expensive since they require specialized equipment and hazardous chemicals and are costly to operate under operating conditions. The hazardous byproducts of chemical processing also result in the pollution of the environment [11]. Additionally, due to their high dipole-dipole interaction, which led to agglomeration, the previous methods had difficulties managing the size distribution of the nanoparticles [12].

Green nanotechnology encourages scientists to employ easier, safer, low-cost, stable, and time-saving plant-mediated schemes for stabilized, uniform particle-size-distributed magnetite nanoparticle synthesis [13]. Recently an alternating approach to green-synthesized nanocomposite adsorbent has gained attention over the standard techniques previously discussed [14]. Phytochemicals contained in plant extracts serve as reducing and capping agents when nanoparticles are produced. The popularity of plant-mediated green synthesis is supported by the rise in research publications over the past few decades. The plant extract-coated green-synthesized adsorbent has been explored in wide dimensions of research over the last few decades [11]. Furthermore, numerous phytochemicals present in the plant extracts, which act as both reducing and capping agents during the formation of NPs [9]. The increase in the number of research articles in recent decades substantiates the popularity of plant-mediated green synthesis of NPs.

Previous research indicates that extracts from different plant components, such as *Lathyrus sativus* peel extract [15], *Azadirachta indica* [16], *Rhus coriaria* peel extract [17], *Moringa oleifera* [18], *Ficus carica* fruit extract [19], *Syzygium aromaticum* extracts [19], etc have been explored for Fe_3O_4-NP manufacture. There have been no reports on the synthesis of FeO_4-NPs employing jackfruit leaf extract. The national fruit of Bangladesh is the jackfruit (*Artocarpus heterophyllus*). The mulberry family (Moraceae), which includes the jackfruit, is indigenous to areas of South and Southeast Asia [20]. Numerous phytochemical elements, including flavonoids, alkaloids, sugars, proteins, carbohydrates, tannins, phenols, and amino acids, are abundant in the jackfruit leaf extract and function as capping, reducing, and stabilizing agents [21]. The phytochemicals in jackfruit leaf extract may be able to decrease metallic salts into their equivalent NPs. We assumed that the phytochemicals present in jackfruit leaf extract could be used as a reducing agent for the reduction of metallic salts into their respective NPs. The phytochemicals are important because they prevent the produced nanoparticles from aggregating and help to stabilize them.

Very few comparative studies of the assessment of physicochemical properties of jackfruit leaf extract synthesized magnetite with chemically synthesized magnetite focus on the difference in crystallinity, phase purity, surface morphology, and surface functional groups. This work is innovative considering the comparative structural characteristics of magnetite preparation using the traditional chemical method and synthesizing using jackfruit leaf extract. This study aimed to compare the physicochemical characteristics of green-synthesized and chemically synthesized magnetite nanoparticles to usher in a new era of choosing suitable synthetic techniques for environmental remediation.

2. Materials and Methods

2.1. Materials

This study used all analytical-grade reagents, including ferrous sulfate heptahydrate ($FeSO_4 \cdot 7H_2O$), ferric chloride hexahydrate ($FeCl_3$ $6H_2O$), and ammonium hydroxide (25% w/v), which were provided by Sigma Aldrich, Chemie GmbH, USA. Sodium hydroxide (Merck: 99.8%) and hydrochloric acid (37%, Merck: 99.9%) were used without further purification. The solutions were prepared using deionized water (DI).

2.2. Preparation of Plant Extract

The study collected the leaves of *Artocarpus heterophyllus* (jackfruit) from the University of Rajshahi, Bangladesh campus. Distilled water (DW) is used for thoroughly washing and oven-drying at 60 ℃ for 24 hours. Approximately 40 g of ground powdered leaves were heated in 300mL of DW for 40 min. The jackfruit leaf extract (JLE) was stored at 4 ℃ after cooling and filtering for further use.

2.3. Preparation of Chemically Synthesized Magnetite

50mL of 0.5 M HCl was used to dissolve $FeCl_3.6H_2O$ and $FeSO_4.7H_2O$ with 1:2 molar ratio (Fe^{2+}/Fe^{3+}). The mixture was then aggressively agitated at 500 rpm at 80 ℃ using a magnetic stirrer. Following a dropwise addition of NaOH (5.0 M) solution till pH 11, the black precipitate of Fe_3O_4 was collected and oven-dried at 75 ℃ for the whole night.

$FeCl_3.6H_2O$ and $FeSO_4.7H_2O$ with a 1:2 molar ratios (Fe^{2+}/Fe^{3+}) were dissolved in 50mL of 0.5 M HCl and stirred vigorously on a magnetic stirrer at 500 rpm at 80 ℃. Then NaOH (5.0 M) solution was added dropwise until pH 11, and the black precipitate of Fe_3O_4 was collected through an overnight oven dried at 75 ℃ [22].

2.4. Preparation of Green Synthesized Magnetite

50mL of DI was mixed with 1:2 molar ratios of (Fe^{2+}/Fe^{3+}) after 30 minutes of stirring. Extract from jackfruit leaves (40mL) was added. To achieve the final black precipitate of Fe_3O_4, after adding 0.1 M of NaOH gradually until the pH reached 11, the precipitation process was stirred for approximately three to four hours at 80 ℃. Then meticulously repeated the washing process 3-4 times with DI, ensuring the purity of the nanoparticles, followed by centrifugation to obtain the nanoparticles, which were then oven-dried at 55 ℃ overnight [9].

2.5. Characterization

The analysis of XRD was carried out on a spectrometer (D/tex Ultra 250, H) with Cu-Kα radiation. FT-IR spectra were recorded by an ATR-FTIR machine (PerkinElmer Spectrum Two, UK), and SEM and EDS analysis was done with a Joel, model JSM IT800. A Horiba analyzer (SZ-100, Japan) was used to measure zeta potential. An analysis of dynamic light scattering (DLS) was performed using the Horiba analyzer (SZ-100, Japan). TGA-DTA analysis was done with a simultaneous thermal analyzer (STA 8000). Origin 2024 software was used to prepare all graphical presentations.

3. Results and Discussion

3.1. Formation of Magnetite Nanoparticles (Fe_3O_4-NPs)

The formation of Fe_3O_4-NPs was initially identified visual observation. During the process of synthesis, the color of the reaction mixture was changed from dark brown to black [23], which was the key sign of the formation of Fe_3O_4-NPs (Figure 1a and b). The color change was due to the interaction between the phytochemicals and iron salts. In case of green synthesized magnetite, the phytochemicals present in the jackfruit leaf extract, such as phenolic compounds and flavonoids, are known to form complexes with transition metal ions including Fe(II) and Fe(III), often resulting in visible color changes due to charge transfer interactions. The phenolic hydroxyl groups donate electrons to ferric and ferrous ions, reducing them and aiding in the nucleation and stabilization of magnetite (Fe_3O_4) [24]. Furthermore, these biomolecules capping agents, preventing the agglomeration and enhancing stability of the NPs in aqueous media.

A possible formation mechanism of magnetite nanoparticles by this green method is as follows in Figure 1a. In the reaction medium, $FeCl_3 \cdot 6H_2O$ and $FeCl_2 \cdot 4H_2O$ Coexist, and JL (Jackfruit leaf extract) is present in a single aqueous phase. The C=O of the carboxylic group in leaf extract chelated with Fe^{3+} and Fe^{2+} to form ferric and ferrous protein. The OH- ions generated from NaOH would be involved in the reaction. A competition between COO- Fe^{3+} and COO-Fe^{2+} bonds and the formation of HO-Fe^{3+} and OH-Fe^{2+} bonds, and a result in the formation of ferric hydroxide, $Fe(OH)_3$, and ferrous hydroxide, $Fe(OH)_2$. The formation of ferric hydroxide and ferrous hydroxide forms a shell core structure. Ferric hydroxide and ferrous hydroxide in core dehydrated ($-H_2O$) forming magnetite (Fe_3O_4) nanoparticle crystals. The shell of leaf extract chains attached to the Fe_3O_4 surface through chelation of COO-Fe^{3+} and COO-Fe^{2+} at the end of the reaction, Fe_3O_4 nanoparticle crystals were capped and stabilized by phenolic compounds of leaf extract [25]. Since green synthesis magnetite employed leaf extract containing biomolecules it is more stabilized than chemically synthesized magnetite [26].

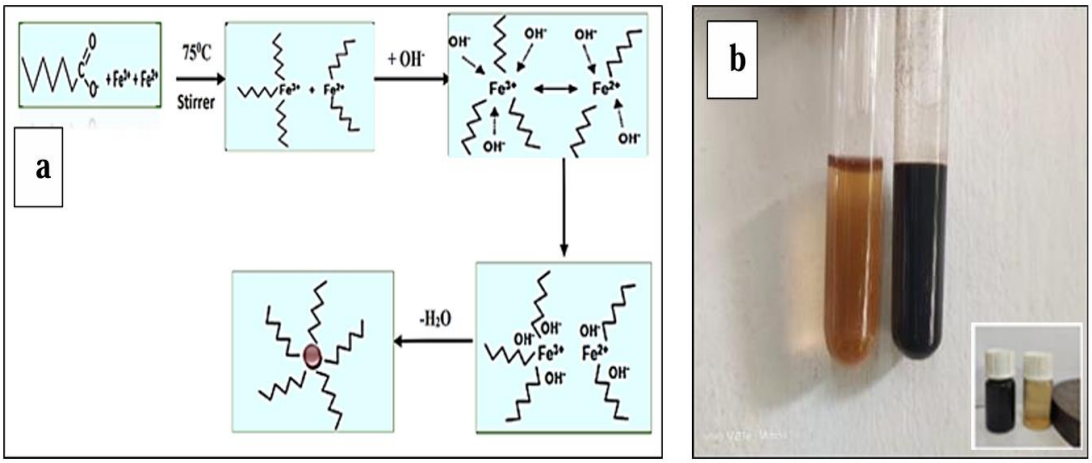

Figure 1. *Mechanism for the formation (a) and visible color change with magnetic attraction of magnetite (b).*

3.2. XRD Analysis

The X-ray diffraction (XRD) pattern of green-produced magnetite, maghemite, and GSMMN adsorbents was displayed in (Figure 2), which also illustrated the crystalline structure of GSMMN. The planes (220), (311), (400), (511), and (440) may be identified by the five distinct diffraction peaks at 30.24 °, 35.51 °, 43.32 °, 57.12 °, and 62.76 °, respectively, in chemically synthesized magnetite (Figure 2a), and for green synthesized magnetite (Figure 2b), the diffraction peaks at 30.25 °, 35.54 °, 43.32 °, 56.77 °, and 62.70 °, respectively, reflect the five planes (220), (311), (400), (511), and (440). These peaks are closely related to the crystalline phase with the cubic pattern of magnetite (JCPDS file no. 19-0629) [9]. The absence of additional peaks in the XRD diagram suggested the NPs' purity. The plane 311 is in the predominant orientation since it is in a more intense position. Debye-Scherrer's equation was utilized to measure the average crystalline size of the adsorbent GSMMNs in Eq. 1 [15].

$$D = \frac{k\lambda}{\beta \cos\theta} \quad (1)$$

The value of k, commonly referred to as Scherer's constant, is 0.9, where D (nm) is the mean crystalline size. Where λ is the wavelength of Cu K (0.154nm), β is the full width at half maximum intensity (FWHM) in radians, and θ ° is the Bragg angle (°) and half diffraction angle of 2θ °. The XRD pattern of nanocomposites was observed in the decreasing peak intensity in some planes due to the successful coating of silica. For the chemical synthesis and green synthesis approaches, the average magnetite nanoparticle sizes were 8.4nm and 11nm, respectively. Because the green synthesis approach uses reducing phytochemicals in leaf extract, the average particle size determined by this method is less than that of the conventional method [27].

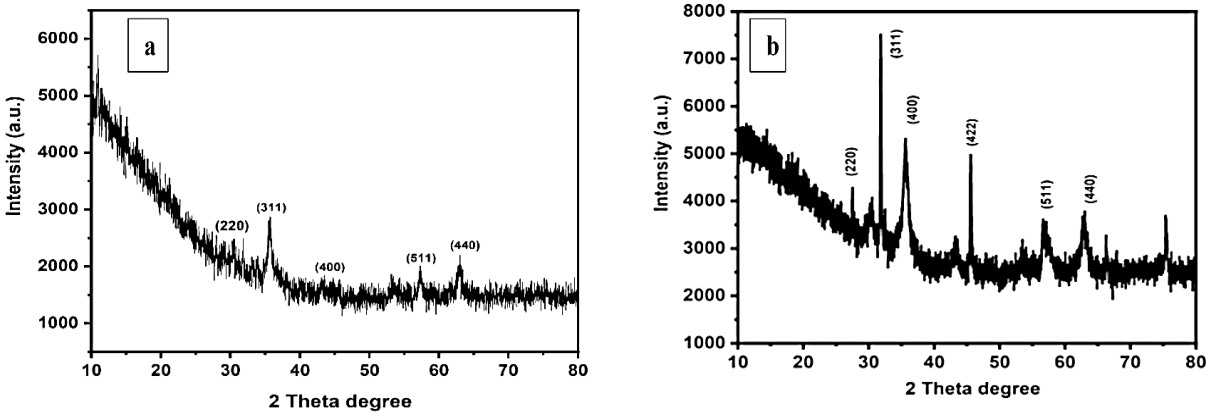

Figure 2. *XRD spectra of chemically spectra of chemically synthesized (a) and green synthesized (b) magnetite nanoparticles.*

3.3. FT- IR Analysis

The presence of JL extract as the capping and reducing agent that stabilized the green-produced magnetite was demonstrated by the Fourier Transmission Spectroscopy (FT-IR) analysis [15]. The FT-IR spectra of chemically and green synthesized magnetite are given in (Figure 3a, b). The stretching vibration of -OH was 3413 cm^{-1} for chemically synthesized magnetite. The slightly shifted absorption band to the lower frequency of 3410 cm^{-1} for green synthesized magnetite caused by the presence of the phenolic -OH group resulted in increased interaction [15]. Additionally, the green-synthesized magnetite's wider peak of the -OH group (Figure 3b) indicated a large surface area of nanoparticles appropriate for the adsorption [9]. The prominent peak observed at 568 cm^{-1}, 640 cm^{-1}, and 582 cm^{-1} for both chemical synthesis methods and green coated Fe_3O_4 NPs is thought to be caused by the stretching vibration mode associated with the metal-oxygen Fe-O linkages in Fe's crystalline lattice. They are visible in all magnetite nanoparticle formations [8]. In the green-synthesized Fe_3O_4 NPs samples, a wide band between 1621 and 1649 cm^{-1} may be a result of C=O stretching vibration [16]. It was further demonstrated that the hydroxyl group, which stands for the O-H stretching vibration, is the source of the peaks in the 3442 cm^{-1} to 3596 cm^{-1} range. These peaks were more prominent for the Fe_3O_4 NPs samples that had a higher proportion of leaf extract. The peak for the C=O and C-O stretching vibrations shifted from 1646 cm^{-1} to 1644 cm^{-1} and from 1052 cm^{-1} to 1065 cm^{-1} when leaf extract was used to cover the green-synthesized magnetite. When leaf extract was employed for covering the green-synthesized magnetite, the peak for the C=O and C-O stretching vibrations shifted from 1646 cm^{-1} to 1644 cm^{-1} and from 1052 cm^{-1} to 1065 cm^{-1}. The FT-IR results confirmed the stability of green-synthesized magnetite due to the successful coating of

leaf extract as stabilizing and capping agents [29].

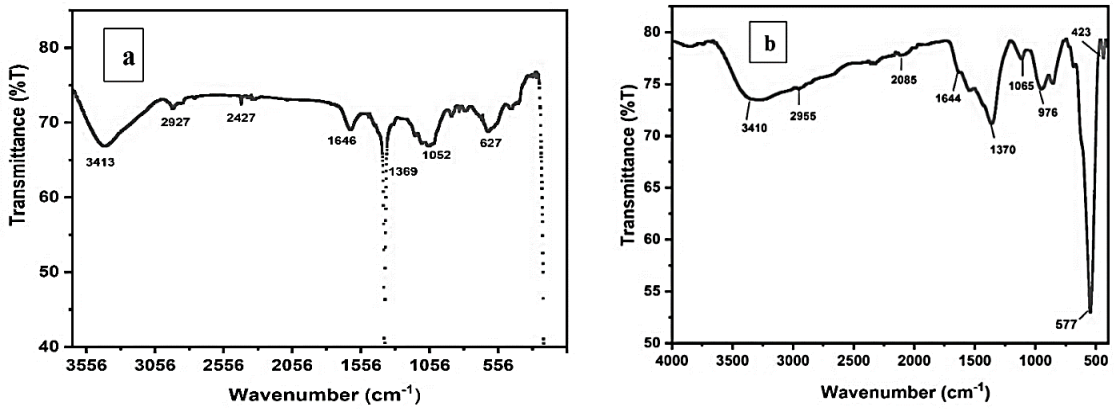

Figure 3. *FT-IR spectra of chemically synthesized (a) and green synthesized (b) magnetite nanoparticles.*

3.4. SEM-EDS Analysis

Scanning Electron Microscopy (SEM) analysis of the chemically and green-synthesized Fe_3O_4 NPs was used to analyze their surface shape, as seen in Figure 4. The surface of chemically synthesized magnetite was irregular in shape and had some holes suitable for the adsorption of heavy metals (Figure 4a). Figure 4a illustrates the morphology of chemically synthesized magnetite nanoparticles, which exhibit a more compact, relatively uniform, and angular structure. The particles appear densely packed, with clearer edges and moderately defined grain boundaries, indicating a high degree of crystallinity and homogeneity. This morphology is typical of conventional co-precipitation synthesis [28].

However, the SEM images of green-synthesized magnetite in (Figure 4b) showed a somewhat agglomerated structure. The particles appear more irregular and loosely aggregated with a comparatively porous and fluffy texture. This morphological difference can be attributed to the capping and stabilizing action of phytochemicals present in the leaf extract (e.g., polyphenols, flavonoids), which influence the nucleation and growth process during synthesis. The bio-organic matrix likely leads to steric hindrance and variation in crystal growth, resulting in less-defined shapes and reduced aggregation compactness. Moreover, the presence of organic residues may partially obscure the surface details, contributing to a blurred appearance in SEM images (Figure 4b) [27]. In this case, the NPs' strong van der Waals forces and inter-particle agglomeration or aggregation lead to a greater surface area that has greater potential for the adsorption of heavy metals than the chemically synthesized method [28]. These differences confirm the influence of synthesis routes on particle morphology, where the green method introduces natural variability due to biological compounds, whereas chemical methods offer more control and uniformity. Despite the irregular morphology, the green synthesized particles may offer enhanced surface functionality and adsorption potential due to higher surface area and porosity [27]. Additionally, the green-synthesized magnetite's higher surface area facilitated greater attraction for heavy metals adsorbed shown in Figure 4b. The magnetite nanoparticles that are synthesized using the traditional chemical technique are very large in diameter and are not evenly distributed (Figure 4a).

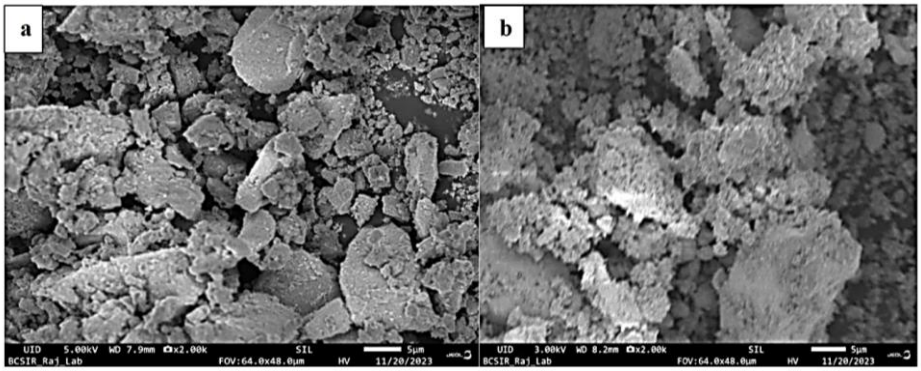

Figure 4. *SEM images of chemically synthesized (a) and green synthesized (b) magnetite nanoparticles.*

Figure 5 shows the elemental mapping of the components found in both chemically and green-synthesized Fe_3O_4 NPs, as shown by the Energy Dispersive X-Ray Spectroscopy (EDS) spectra. The image from (Figure 5a) confirmed the presence of elements Fe and O in chemically synthesized magnetite. Chemically synthesized Fe_3O_4 NPs were validated by the presence of signals at 0.7, 6.4, and 7 keV for elemental iron and the peak at 0.5 keV for elemental oxygen [26]. The elemental composition of the nanoparticle was Fe (77.46%) and O (22.54%) [27]. While the presence of signals at 0.5, 6.7, and 7 keV for elemental iron proved the green-synthesized Fe_3O_4, the presence of carbon, which came from the leaf extract's biomolecules, was validated by the peaks at 0.5 keV for elemental oxygen and 0.3 keV [15]. The green-synthesized magnetite nanoparticles were composed of the elements O (20.68%), Fe (72%), and C (7.32%) [28]. The purity of the nanoparticles was indicated by the absence of additional signals. Consequently, the SEM-EDS data confirmed that the green-synthesized Fe_3O_4 nanoparticles were incorporated with biomolecules.

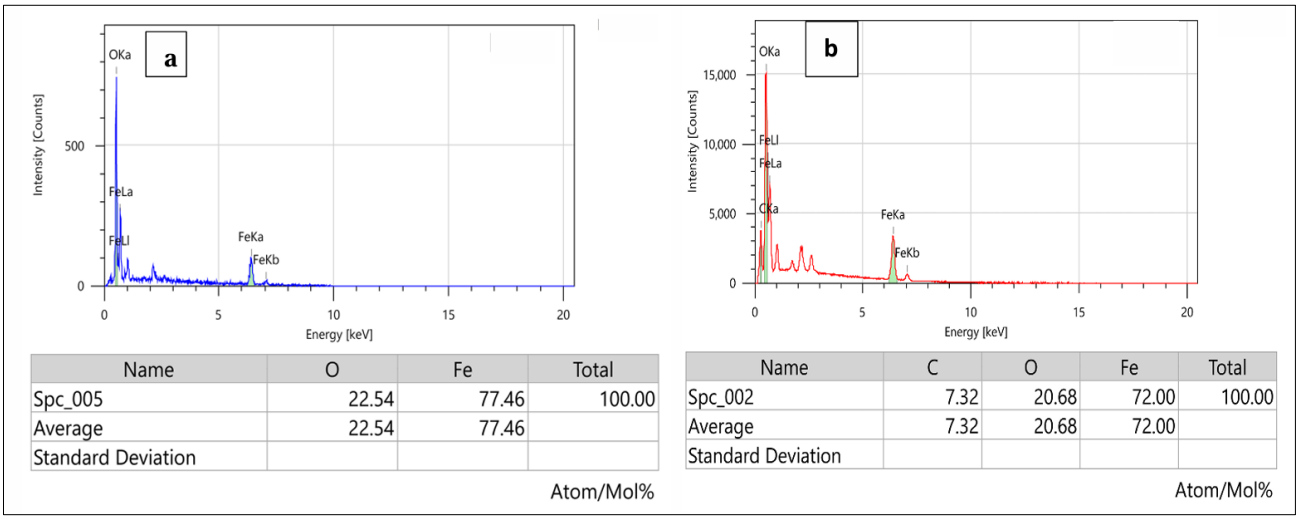

Name	O	Fe	Total
Spc_005	22.54	77.46	100.00
Average	22.54	77.46	
Standard Deviation			

Atom/Mol%

Name	C	O	Fe	Total
Spc_002	7.32	20.68	72.00	100.00
Average	7.32	20.68	72.00	
Standard Deviation				

Atom/Mol%

Figure 5. *EDS spectra of chemically synthesized magnetite (a) green synthesized magnetite (b) nanoparticles.*

3.5. TGA-DTA Analysis

The synthesized nanoparticles' thermal stability, breakdown temperature, and rate were examined employing thermogravimetric analysis-differential thermal analysis (TGA-DTA) [29]. To evaluate the thermal stability of magnetite nanoparticles produced using the environmentally friendly and chemically synthesized method depicted in (Figure 6), TGA-DTA analysis was carried out in the temperature range of 30 to 800 ℃. From (Figure 6a), it was observed that the chemically synthesized magnetite underwent an initial 2.67% weight loss, and the green-synthesized magnetite experienced a 7.4% reduction in weight, which corresponds to the removal of surface water from the nanoparticles at 100 ℃. The decomposition of the capping agents in green-synthesized magnetite was responsible for its higher reduction in weight [29]. According to a TGA analysis, green-synthesized Fe_3O_4 NPs from the aqueous extract were more stable than magnetite NPs created at the same temperature using a conventional chemical method. Here, chemically synthesized magnetite shows three phases of weight loss, while green-synthesized magnetite experiences two phases of weight loss. The second-phase breakdown of bio-organic capping agents in green-produced magnetite was observed between 150 and 400 ℃, with a DTA peak at 298 ℃. In contrast, chemically synthesized magnetite had a second weight loss between 150 and 300 ℃, with a DTA peak at 282 ^{o}C [30]. The green-synthesized magnetite lost less than 1% of its weight between 350 and 800 ℃, demonstrating the purity of the Fe_3O_4 NPs and the nanoparticles' thermal stability at high temperatures, and chemically synthesized magnetite experienced 4.2% weight loss from 300 to 650 ℃ and 2% weight loss from 650 to 800 ℃, suggesting the unstable nature and susceptibility to oxidation. Thus, TGA-DTA analysis suggested that the existence of phytochemicals and the surface modification of green-synthesized magnetite enhance thermal stability more than that of chemically synthesized magnetite [31].

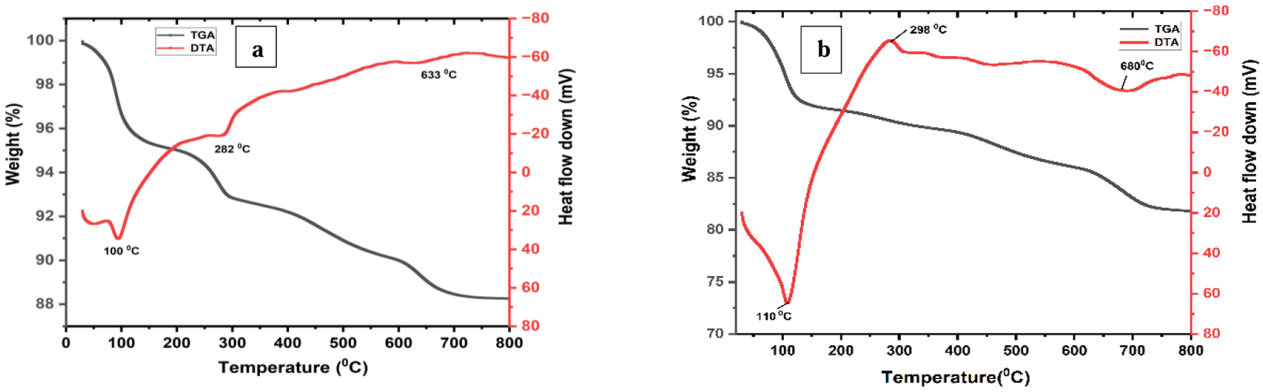

Figure 6. *TGA-DTA curve of chemically synthesized magnetite (a) and green synthesized magnetite (b) nanoparticles.*

3.6. DLS Analysis

Dynamic Light Scattering (DLS) analysis is a widely used technique that uses variations in scattered light intensity caused by Brownian motion to measure the size of nanoparticles in solution [32]. The existence of additional hydrated layers attached to the surface allows hydrodynamic size measurements to typically be larger than the MNPs' actual size measurements. From (Figure 7), it was observed that the chemically synthesized magnetite showed a hydrodynamic size of 158nm, and the green-synthesized magnetite showed that of 150nm. The mechanism governing each synthetic process is responsible for the variations in hydrodynamic size. The formation of a smaller hydrodynamic size for the green-synthesized technique is caused by the presence of biomolecules acting to reduce the particles [33]. Therefore, from the DLS graphs, it can be concluded that the formation of nanoparticles by the green synthesis method results in particle distributions that are a narrower distribution range than the chemical synthesis method [34].

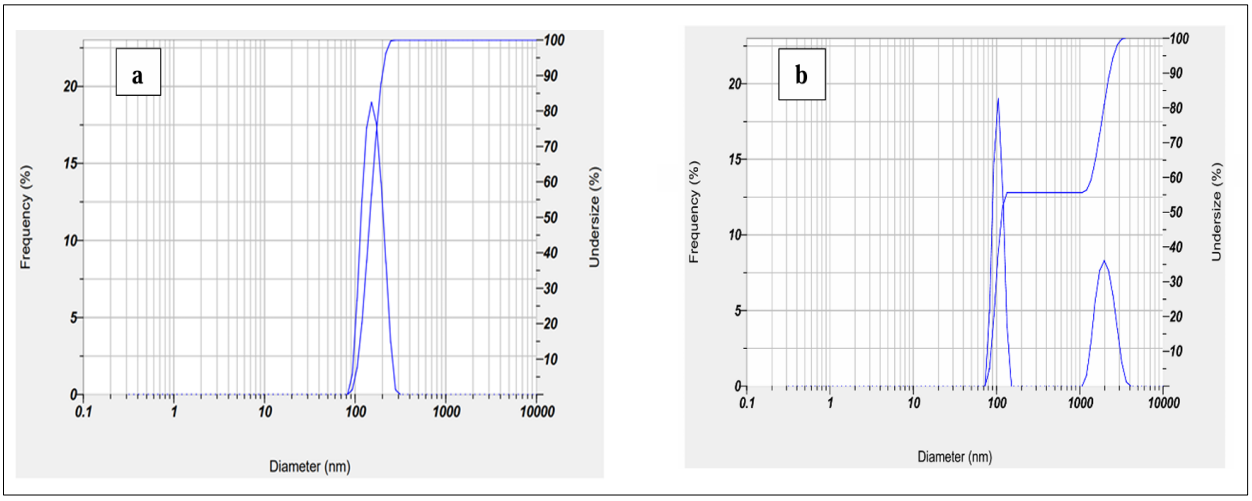

Figure 7. *DLS curve for chemically synthesized magnetite (a) and green synthesized magnetite (b) nanoparticles.*

3.7. Zeta Potential

Zeta potential analysis is a technique used to measure the surface charge or electro-kinetic potential of particles floating in liquid media, typically in colloidal systems. It sheds light on the behavior and stability of colloidal dispersions, including macromolecules, colloidal particles, and nanoparticles. Neutrally charged nanoparticles have zeta potentials between >-10 mV and -30 mV. However, nanoparticles are categorized as strongly cationic and strongly anionic, respectively, if their zeta potentials fall between >-30 mV and <+30 mV [35]. Higher zeta potential levels promote colloidal stability because high charge differences (> ±10 mV) increase interparticle repulsion [36].

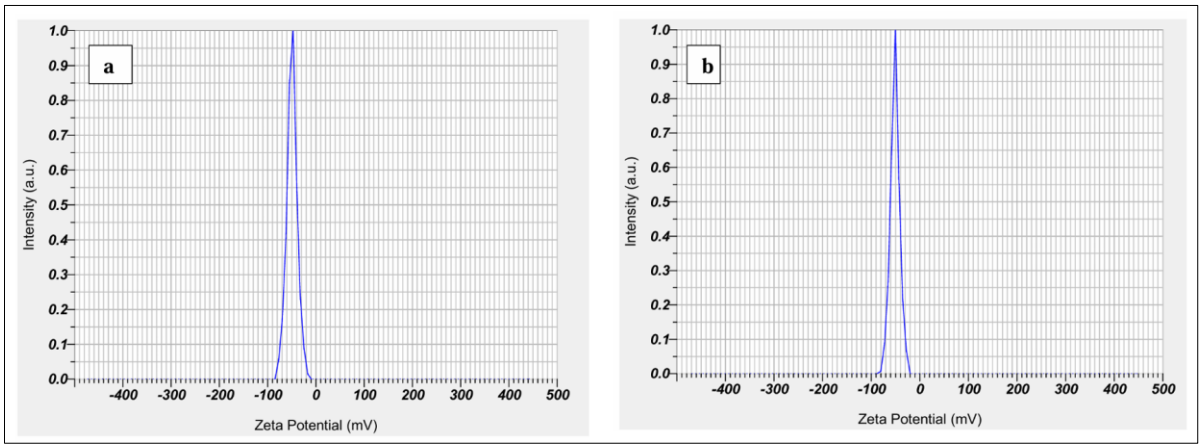

Figure 8. *Zeta potential values of chemically synthesized magnetite (a) and green synthesized magnetite (b) nanoparticles.*

For the Fe_3O_4 nanoparticles made in this work, the chemical synthesis approach had a zeta potential measurement of -47 mV (Figure 8a), and the green synthesis method produced a measurement of -50 mV (Figure 8b). The polydispersity index of chemically synthesized magnetite was 0.41, and that of green-synthesized was 0.3. The inverse relationship between zeta potential and the polydispersity index was demonstrated by the reduction in the polydispersity index as the zeta potential value increased [36]. From the values, it was observed that the zeta potential values are higher in the green-synthesized method than in the conventional method. During the green synthesis process, the surface of the nanoparticles becomes more negatively charged due to the presence of more negatively charged functional groups formed from leaf extract. This keeps the nanoparticles stable and prevents iron particles from aggregating. Based on these results, it can be concluded that green-synthesized Fe_3O_4 nanoparticles are more stable than those produced chemically. They also exhibit reduced particle aggregation and improved colloidal stability [37].

4. Conclusion

This study investigated a green synthesis approach to synthesizing Fe_3O_4 nanoparticles using jackfruit leaf extract as a stabilizing, reducing, and capping agent. This study systematically compared them with Fe_3O_4 nanoparticles produced through a conventional co-precipitation method. Different characterization techniques like XRD, FT-IR, SEM, EDS, TGA, DLS, and zeta potential were employed to compare the characteristic differences between two Fe_3O_4 synthesized by two approaches. The formation of magnetite NPs was confirmed by the color changes, which were due to the interaction between the phytochemicals and iron salts. The mechanism for the formation of magnetite NPs shows more stable NPs can be synthesized by the green synthesis method due to the phytochemicals present in the leaf extract. The XRD analysis showed the average particle size of chemically synthesized magnetite was 11nm, whereas that of green-synthesized magnetite was 8.4nm. FT-IR analysis of green-synthesized magnetite showed the shifting of stretching vibration of C=O and C-O in green-synthesized magnetite from 1646 cm^{-1} to 1644 cm^{-1} and 1052 cm^{-1} to 1065 cm^{-1} after capping with leaf extract. The surface of green-synthesized magnetite was found to have some extent of aggregation. This morphological difference in SEM images is attributed to the capping and stabilizing action of, e.g., polyphenols, flavonoids, present in leaf extract influencing the nucleation and growth process during synthesis. The bio-organic matrix likely leads to steric hindrance and variation in crystal growth, resulting in less-defined shapes and reduced aggregation compactness. The existence of biomolecules in green-produced magnetite was validated by the presence of carbon (C) in the EDS spectrum. The enhanced thermal stability of green-synthesized magnetite was confirmed by the TGA-DTA analysis. The hydrodynamic diameter of chemically synthesized and green-synthesized magnetite was found to be 158nm and 150nm, respectively. The zeta potential of green-synthesized magnetite was found to be -50 mV higher than that of chemically synthesized magnetite (-47 mV). It can be concluded that green-synthesized Fe_3O_4 showed better stability and crystallinity than that of chemically synthesized magnetite. Because the leaf extract's reducing agents serve as a capping agent to keep the nanoparticles stable. Iron oxide nanoparticles can thus be produced in a green route, and their potential usage in many environmental applications—especially the removal of heavy metals from drinking water can be further evaluated.

Abbreviations

NP	Nanoparticles
XRD	X-ray Diffraction Analysis
FT-IR	Fourier Transformation Infrared Spectroscopy
SEM	Scanning Electron Microscopy
EDS	Energy Dispersive

X-ray	Spectroscopy
TGA	Thermogravimetric Analysis
DTA	Differential Thermal Analysis
DLS	Dynamic Light Scattering

Acknowledgments

One of the authors acknowledge the University Grant Commission (UGC), Bangladesh for granting a PhD fellowship.

Author Contributions

Asma Siddiqa: Data collection, Formal analysis, Data curation, Formal analysis, Software and Writing - original draft

Halima Khatun: Formal analysis and Data curation

Golam Mostafa: Conceptualization, Methodology, Supervision, Writing - review & editing

Data Availability Statement

The data that support the findings of this study are offered by the corresponding author upon request.

Conflicts of Interest

The authors declare no conflicts of interest.

References

[1] Zafar, Rabeea, Shanza Bashir, Deedar Nabi, and Muhammad Arshad. "Occurrence and quantification of prevalent antibiotics in wastewater samples from Rawalpindi and Islamabad, Pakistan." Science of The Total Environment 2021, 764, 142596. https://doi.org/10.1016/j.scitotenv.2020.142596

[2] Hossen, Md Anowar, and M. G. Mostafa. "Performance assessment of personal care products industrial effluent treatment plant and its impacts on the environment." Watershed Ecology and the Environment. 2025, 7, 131-143. https://doi.org/10.1016/j.wsee.2025.03.007

[3] Ibrahim, Dalal M., Hanan F. Emrayed, and Asma A. Youssef. "Green and Chemical Synthesis of Magnetite Nanoparticles for Corrosion Inhibition Applications." Iraqi Journal of Applied Physics. 2025, 21(1), 156-160. https://doi.org/index.php/ijap/article/view/357

[4] Sayed, Md Abu, and M. G. Mostafa. "Characterization of textile dyeing effluent and removal efficiency assessment of $Al_2(SO_4)_3$ coagulant." Asian Journal of Applied Science and Technology (AJAST), 2023, 7(3), 195-212. https://doi.org/10.38177/ajast.2023.7314

[5] Mostafa, M. G., Yen-Hua Chen, Jiin-Shuh Jean, Chia-Chuan Liu, and Hsisheng Teng. "Adsorption and desorption properties of arsenate onto nano-sized iron-oxide-coated quartz." Water Science and Technology. 2010, 62(2), 378-386. https://doi.org/10.2166/wst.2010.288

[6] Aktaruzzaman, Md, Sayed MA Salam, and M. G. Mostafa. "Synthesis of Aluminum Oxide Nanoparticle Adsorbents from Waste Aluminum Foil and Assesses Their Efficiency in Removing Lead (II) Ions from Water." Tropical Aquatic and Soil Pollution. 2024, 4(2), 127-142. https://doi.org/journal/tasp/article/view/497

[7] Sun, Xiaohan, Nicolas Alcaraz, Ruirui Qiao, Adrian Hawley, Angel Tan, and Ben J. Boyd. "Magnetically-stimulated transformations in nanostructure of lipid mesophases: Effect of structure of iron oxide nanoparticles." Colloids and Surfaces B: Bio interfaces. 2020, 191, 110965. https://doi.org/10.1016/j.colsurfb.2020.110965

[8] Dowlath, M. J. H., Musthafa, S. A., Khalith, S. M., Varjani, S., Karuppannan, S. K., Ramanujam, G. M.,... & Ravindran, B.. Comparison of characteristics and biocompatibility of green synthesized iron oxide nanoparticles with chemical synthesized nanoparticles. Environmental Research. 2021, 201, 111585. https://doi.org/10.1016/j.envres.2021.111585

[9] Yew, Y. P., Shameli, K., Miyake, M., Kuwano, N., Bt Ahmad Khairudin, N. B., Bt Mohamad, S. E., & Lee, K. X. Green synthesis of magnetite (Fe_3O_4) nanoparticles using seaweed (Kappaphycus alvarezii) extract. Nanoscale research letters. 2016, 11, 1-7. https://doi.org/10.1186/s11671-016-1498-2

[10] Bishnoi, S., Kumar, A., Selvaraj, R.,. Facile synthesis of magnetic iron oxide nanoparticles using inedible Cynometra ramiflora fruit extract waste and their photocatalytic degradation of methylene blue dye. Mater. Res. Bull. 2018, 97, 121-127. https://doi.org/10.1016/j.materresbull.2017.08.040

[11] Vinayagam, Ramesh, Thivaharan Varadavenkatesan, and Raja Selvaraj. "Evaluation of the anticoagulant and catalytic activities of the Bridelia retusa fruit extract-functionalized silver nanoparticles." Journal of Cluster Science. 2017, 28, 2919-2932. https://doi.org/10.1007/s10876-017- 1270-5

[12] Mostafa, M. G., Yen-Hua Chen, Jiin-Shuh Jean, Chia-Chuan Liu, and Yao-Chang Lee. "Kinetics and mechanism of arsenate removal by nanosized iron oxide-coated perlite." Journal of Hazardous Materials. 2011, 187(1-3), 89-95. https://doi.org/10.1016/j.jhazmat.2010.12.117

[13] Rojo, Cynthia, Erico R. Carmona, Lucas Patricio Hernández-Saravia, Aliro Villacorta, Ricard Marcos, Felipe S. Carevic, Venecia Herrera Apablaza, and Ronald Nelson. "Utilization of Orange Peel Waste for the Green Synthesis of Iron Nanoparticles and its Application to Stimulate Growth and Biofortification on Solanum lycopersicum." Waste and Biomass Valorization. 2024, 15(11), 6343-6356. https://doi.org/10.1007/s12649-024-02602-4

[14] Dash, Asiman, Mohammed Tameem Ahmed, and Raja Selvaraj. "Mesoporous magnetite nanoparticles synthesis using the Peltophorum pterocarpum pod extract, their antibacterial efficacy against pathogens and ability to remove a pollutant dye." Journal of Molecular Structure. 2019, 1178, 268-273. https://doi.org/10.1016/j.molstruc.2018.10.042

[15] Dhar, Palash Kumar, Prianka Saha, Md Kamrul Hasan, Md Khairul Amin, and Md Rezaul Haque. "Green synthesis of magnetite nanoparticles using Lathyrus sativus peel extract and evaluation of their catalytic activity." Cleaner Engineering and Technology. 2021, 3,100117. https://doi.org/10.1016/j.clet.2021.100117

[16] Akhtar, Muhammad Shahbaz, Sania Fiaz, Sohaib Aslam, Shinho Chung, Allah Ditta, Muhammad Atif Irshad, Amal M. Al-Mohaimeed et al. "Green synthesis of magnetite iron oxide nanoparticles using Azadirachta indica leaf extract loaded on reduced graphene oxide and degradation of methylene blue." Scientific reports. 2024, 14(1), 18172. https://doi.org/s41598-024-69184-y

[17] Piro, Nzar Shakr, Samir Mustafa Hamad, Ahmed Salih Mohammed, and Azeez Abdullah Barzinjy. "Green synthesis magnetite (Fe_3O_4) nanoparticles from Rhus coriaria extract: a characteristic comparison with a conventional chemical method." IEEE Transactions on NanoBioscience. 2022, 22(2), 308-317. https://doi.org/abstract/document/9810966

[18] Altaf, Sikandar, Rabeea Zafar, Waqas Qamar Zaman, Shakil Ahmad, Khurram Yaqoob, Asad Syed, Asim Jahangir Khan, Muhammad Bilal, and Muhammad Arshad. "Removal of levofloxacin from aqueous solution by green synthesized magnetite (Fe_3O_4) nanoparticles using Moringa olifera: Kinetics and reaction mechanism analysis." Ecotoxicology and environmental safety. 2021, 226, 112826. https://doi.org/10.1016/j.ecoenv.2021.112826

[19] Tahir, Aberah, Adnan Saeed, Iqra Ramzan, Sardar Sikandar Hayat, Waqar Ahmad, Samia Naeem, Marina Afzal, Aiman Mukhtar, Tahir Mehmood, and Babar Shahzad Khan. "Mechanism for the formation of magnetite iron oxide nanostructures by Ficus carica dried fruit extract using green synthesis method." Applied Nanoscience. 2021, 11(6), 1857-1865. https://doi.org/10.1007/s13204-021-01860-1

[20] Gaminda, K. A. P., Thomas, I. B. K., Lakmauri, P., Abeysinghe, T., Jayasinghe, C., & Senthilnithy, R. Green synthesis of iron nanoparticles using Syzygium aromaticum extracts and their applications: Nitrate removal, malachite green degradation and antibacterial activity. Environmental Nanotechnology, Monitoring & Management. 2024, 21, 100925. https://doi.org/10.1016/j.enmm.2024.100925

[21] Ramesh, A. V., Dharmasoth Rama Devi, Satish Mohan Botsa, and K. Basavaiah. "Facile green synthesis of Fe_3O_4 nanoparticles using aqueous leaf extract of Zanthoxylum armatum DC. for efficient adsorption of methylene blue." Journal of Asian Ceramic Societies. 2018, 6(2), 145-155. https://doi.org/10.1080/21870764.2018.1459335

[22] Pandey, Anmol, Ashish Bhagat, and Bhaskar Bhaduri. "Synthesis of magnetite nanoparticles deposited on heat-treated graphitic carbon nitride for the removal of methylene blue dye molecules by adsorption." Chemical Engineering Communications. 2025, 212(6), 922-949. https://doi.org/10.1080/00986445.2024.2445225

[23] Chen, Wei, Jing Wu, Xiulan Weng, Gary Owens, and Zuliang Chen. "One-step green synthesis of hybrid Fe-Mn nanoparticles: Methodology, characterization and mechanism." Journal of Cleaner Production. 2022, 363, 132406. https://doi.org/10.1016/j.jclepro.2022.132406

[24] Kirubakaran, Dharmalingam, Jamith Basha Abdul Wahid, Natchimuthu Karmegam, Ravisankar Jeevika, Latha Sellapillai, Manickam Rajkumar, and K. J. SenthilKumar. "A comprehensive review on the green synthesis of nanoparticles: advancements in biomedical and environmental applications." Biomedical Materials & Devices. 2025, 1-26. https://doi.org/10.1007/s44174-025-00295-4

[25] Rasool, Akhtar, Sudewi Sri, Muhammad Zulfajri, and Fransiska Sri Herwahyu Krismastuti. "Nature inspired nanomaterials, advancements in green synthesis for biological sustainability." Inorganic Chemistry Communications. 2024, 112954. https://doi.org/10.1016/j.inoche.2024.112954

[26] Amin, Fozia, Fozia, Baharullah Khattak, Amal Alotaibi, Muhammad Qasim, Ijaz Ahmad, Riaz Ullah et al. "Green synthesis of copper oxide nanoparticles using Aerva javanica leaf extract and their characterization and investigation of in vitro antimicrobial potential and cytotoxic activities." Evidence-Based Complementary and Alternative Medicine. 2021, 1,5589703. https://doi.org/10.1007/978-981-33-6915-3

[27] Kummara, Sivaiah, Mrityunjaya B. Patil, and Tiewlasubon Uriah. "Synthesis, characterization, biocompatible and anticancer activity of green and chemically synthesized silver nanoparticles-a comparative study." Biomedicine & Pharmacotherapy. 2016, 84, 10-21. https://doi.org/10.1016/j.biopha.2016.09.003

[28] Yusefi, Mostafa, Kamyar Shameli, Ong Su Yee, Sin-Yeang Teow, Ziba Hedayatnasab, Hossein Jahangirian, Thomas J. Webster, and Kamil Kuča. "Green synthesis of Fe_3O_4 nanoparticles stabilized by a Garcinia mangostana fruit peel extract for hyperthermia and anticancer activities." International Journal of Nanomedicine. 2021, 2515-2532. https://doi.org/10.2147/IJN.S284134

[29] John, K. Smitha, M. S. Parvathi, A. S. Krishna, Arya Sidharth, and T. Geetha. "Ocimum gratissimum mediated green synthesised iron oxide nanoparticles as a plausible nanofertilizer for peanut plant (Arachis hypogaea)." Discover Applied Sciences. 2024, 6(10), 542. https://doi.org/10.1007/s42452-024-06241-1

[30] Juturu, Rajesh, Raja Selvaraj, and Vytla Ramachandra Murty. "Efficient removal of hexavalent chromium from wastewater using a novel magnetic biochar composite adsorbent." Journal of Water Process Engineering. 2024, 66, 105908. https://doi.org/10.1016/j.jwpe.2024.105908

[31] Mhammedsharif, Renjbar Muksy, Parwin Jalal Jalil, Nzar Piro, Ahmed Salih Mohammed, and Peyman K. Aspoukeh. "Myco-generated and analysis of magnetite (Fe_3O_4) nanoparticles using Aspergillus elegans extract: A comparative evaluation with a traditional chemical approach." Heliyon. 2024, 10(11). https://doi.org/10.1016/j.heliyon.2024.e31352

[32] Vinayagam, Ramesh, Chenxi Zhou, Shraddha Pai, Thivaharan Varadavenkatesan, Manoj Kumar Narasimhan, Selvaraju Narayanasamy, and Raja Selvaraj. "Structural characterization of green synthesized magnetic mesoporous Fe_3O_4NPs@ ME." Materials Chemistry and Physics. 2021, 262,124323. https://doi.org/10.1016/j.matchemphys.2021.124323

[33] Vora, R., Patel, H., & Parekh, K.. Environment friendly synthesis of Fe_3O_4 nanoparticles using moringa oleifera seed/pulp extract and their application for dye wastewater treatment. Advances in Natural Sciences: Nanoscience and Nanotechnology. 2024, 16(1), 015001.
https://doi.org/10.1088/2043-6262/ad9ff2

[34] Kuznowicz, Maria, Artur Jędrzak, Tomasz Rębiś, and Teofil Jesionowski. "Biomimetic magnetite/polydopamine/β-cyclodextrins nanocomposite for long-term glucose measurements." Biochemical Engineering Journal. 2021, 174,108127.
https://doi.org/10.1016/j.bej.2021.108127

[35] Kumar, Brajesh, Kumari Smita, Luis Cumbal, Alexis Debut, Salome Galeas, and Victor H. Guerrero. "Phytosynthesis and photocatalytic activity of magnetite (Fe_3O_4) nanoparticles using the Andean blackberry leaf." Materials Chemistry and Physics. 2016, 179, 310-315.
https://doi.org/10.1016/j.matchemphys.2016.05.045

[36] Das, Chanchal, Subhadeep Sen, Tejinder Singh, Tanmoy Ghosh, Subha Sankar Paul, Tae Wan Kim, Seob Jeon, Dilip K. Maiti, Jungkyun Im, and Goutam Biswas. "Green synthesis, characterization and application of natural product coated magnetite nanoparticles for wastewater treatment." Nanomaterials. 2020, 10(8), 1615.
https://doi.org/10.3390/nano10081615

[37] Kahani, Seyed Abolghasem, and Zahra Yagini. "A comparison between chemical synthesis magnetite nanoparticles and biosynthesis magnetite." Bioinorganic Chemistry and Applications. 2014, (no. 1), 384984.
https://doi.org/10.1155/2014/384984